Author Manuscript

Author Manuscript

Author Manuscript

Author Manuscript

HHS Public Access

Author manuscript

Acad Radiol. Author manuscript; available in PMC 2017 September 26.

Published in final edited form as:

Acad Radiol. 2014 June ; 21(6): 726–732. doi:10.1016/j.acra.2014.02.005.

Optimal Timing and Diagnostic Adequacy of Hepatocyte Phase Imaging with Gadoxetate-Enhanced Liver MRI

Mustafa R. Bashir, MD, **Steven R. Breault, MD**, **Ryan Braun, MD**, **Richard K. Do, MD, PhD**, **Rendon C. Nelson, MD**, and **Scott B. Reeder, MD, PhD**

Department of Radiology, Duke University Medical Center, DUMC 3808, Durham, NC 27710 (M.R.B., S.R.B., R.C.N.); Department of Radiology, Rush University Medical Center, Chicago, IL 60612 (R.B.); Department of Radiology, Memorial Sloan-Kettering Cancer Center, New York, NY 10065 (R.K.D.); and Departments of Radiology, Medical Physics, Biomedical Engineering, and Medicine, University of Wisconsin, Madison, WI 53792 (S.B.R.)

Abstract

Rationale and Objectives—To evaluate clinical and imaging features associated with adequacy of the hepatocyte phase (HP) in gadoxetate disodium–enhanced liver magnetic resonance imaging (MRI) in patients without chronic liver disease (CLD).

Materials and Methods—This was a retrospective institutional review board–approved study of 97 patients who underwent liver MRI examinations with gadoxetate disodium and had no history of CLD. Available late dynamic and HP sequences (3–20 minutes postinjection) were independently analyzed by four radiologists for perceived image adequacy and level of biliary enhancement. Signal intensity ratios (SIRs) of liver/inferior vena cava (IVC), liver/spleen, and liver/muscle were measured. The Spearman ρ and receiver operating characteristic analyses were performed correlating various factors with HP adequacy. A rule for predicting HP adequacy was also derived and tested to determine whether overall examination time could be shortened.

Results—A visually adequate HP was observed in 12% of subjects by 10 minutes, 80% by 15 minutes, and 93% by 20 minutes. An $SIR_{liver/\ IVC} > 1.8$ was the imaging feature that had the strongest correlation with an adequate HP ($\rho = 0.813$, $P < .001$), and was more predictive of adequacy of the HP than the time postinjection ($\rho = 0.5$, $P < .001$). The time at which an adequate HP was first observed did not correlate with any tested demographic or laboratory values. Stopping imaging when an $SIR_{liver/IVC} > 1.8$ would have successfully reduced mean postcontrast time to 15:39 ± 4:02 from 20:00 ($P < .001$), although maintaining HP adequacy.

Conclusions—Most patients without CLD undergoing gadoxetate-enhanced liver MRI achieve adequate HP at 20 minutes. However, a shorter postcontrast stopping time can be used in most patients.

Keywords

Gadoxetate disodium; gadoxetic acid; hepatocyte phase; hepatobiliary

Address correspondence to: M.R.B. mustafa.bashir@duke.edu.

Disclosures: MRB is a consultant to Bayer Healthcare, the makers of gadoxetate disodium. SRB, RB, RKD, and RCN have nothing to disclose.

Author Manuscript Author Manuscript Author Manuscript Author Manuscript

Gadoxetate disodium is becoming a well-established contrast agent for contrast-enhanced magnetic resonance imaging (MRI) of the noncirrhotic liver for the detection of metastatic disease and the evaluation of focal lesions (1–8). In particular, hepatocyte phase (HP) imaging with this agent along with an optimized imaging protocol has been shown to provide high-resolution imaging with strong liver-to-lesion contrast and lesion conspicuity (9–12). At many centers, gadoxetate-enhanced MRI has become the study of choice for the detection of hepatic metastases from a variety of primary tumors.

Although most publications describe the performance of the HP performed at 20 minutes postinjection, there remains debate as to whether shorter imaging times can be used for the delayed phase without compromising image quality (13–15). In particular, the use of 10-minute postinjection HP image sets has been described, with excellent performance for the detection of focal lesions (14,16). Thus the ideal timing of the HP is unclear.

Importantly, the rapidity and strength of hepatic gadoxetate uptake is strongly dependent on the functional status of the liver, although definitive laboratory and clinical predictors of uptake are lacking. In addition, MRI examinations using gadoxetate often require more time than those obtained with other gadolinium-based contrast agents, and the total examination time depends partly on the delay for HP imaging. For this reason, a prediction rule for stopping a gadoxetate-enhanced MRI before the 20-minute postinjection time point may be helpful.

The purpose of this study was to evaluate clinical and imaging features associated with adequacy of the HP in gadoxetate disodium–enhanced liver MRI in patients without chronic liver disease (CLD).

MATERIALS AND METHODS

This was an Health Insurance Portability and Accountability Act (HIPAA)-compliant retrospective study, approved by our institutional review board. The requirement for informed consent was waived by the institutional review board.

A search of the electronic medical record at a single institution was performed for all consecutive patients who underwent gadoxetate-enhanced liver MRI at our institution between February 28, 2012 and August 21, 2012. Imaging protocols included postcontrast three-dimensional T1-weighted sequences obtained 3–6 minutes postcontrast injection, at 6–15 minutes postinjection, and 15–25 minutes postinjection. Precise timing and number of postcontrast sequences were variables because of the variability of acquisition time for T2-weighted and diffusion-weighted sequences obtained between T1-weighted acquisitions, as well as patient and technologist factors. Additional inclusion criteria included at least one postcontrast T1-weighted acquisition obtained at 3–15 minutes and at least one at 15–25 minutes after contrast media injection, and T1-weighted image data set obtained using identical protocols on identical MRI systems (detailed subsequently). Patients with a history of CLD, including cirrhosis, viral hepatitis, nonalcoholic steatohepatitis, primary sclerosing cholangitis, or primary biliary cirrhosis were excluded ($n = 28$). Patients without a documented history of CLD but with imaging findings of CLD or portal hypertension were

Author Manuscript Author Manuscript Author Manuscript Author Manuscript

also excluded, in particular liver contour nodularity ($n = 1$) and gastroesophageal varices ($n = 1$). Ultimately, 97 patients with 240 corresponding HP data sets comprised the study population. Patient demographics and laboratory values obtained within 4 weeks of imaging were collected.

All included image data sets were obtained on a 3 T MRI system (Skyra; Siemens Healthcare, Erlangen, Germany) using a three-dimensional T1-weighted dual-echo acquisition, postprocessed with a Dixon water–fat separation algorithm (17,18). Only the water-only image sets were reviewed. Additional parameters included repetition time 3.9–4.2 milliseconds, source in/opposed phase echo times 1.2/2.5 milliseconds, flip angle 9°, acquisition matrix 288 × 230–288 × 72 slices, section thickness 4 mm, field of view 38–40 × 27–40 cm, receiver bandwidth 1020 Hz/pixel, and number of signal averages 1. All patients received a standard dose of 10 mL of gadoxetate disodium (Eovist; Bayer Healthcare, Wayne, NJ) intravenously at 2 mL/seconds followed by a 20 mL saline chaser also injected at 2 mL/seconds. Nonweight-based dosing was used clinically as this has been shown to increase the average amount of contrast enhancement compared to weight-based dosing of 0.025 mmol/kg (15,19). The time between data set acquisition and contrast media administration was calculated using Digital Imaging and Communications in Medicine (DICOM) header data.

Image sets were randomized so that data sets from the same examinations were reviewed nonconsecutively, and were also randomized with respect to timing of acquisition. In addition to anonymization, all information regarding image set timing was removed. Four fellowship-trained abdominal radiologists who were faculty at four different academic institutions, each with 3–8 years of postfellowship experience with abdominal MRI, independently evaluated HP data sets meeting the previously mentioned criteria in a fully blinded manner. All radiologists had at least 3 years experience interpreting gadoxetate-enhanced MRI.

Readers were asked to grade each data set according to the following features: (1) Adequacy of HP/timing for the specific task of evaluation for focal liver lesions (Grade 0, nondiagnostic; Grade 1, suboptimal; Grade 2, diagnostic; and Grade 3, ideal), (2) The presence and delayed phase intensity of any focal liver lesions (Grade 0, no lesion; Grade 1, hypointense lesion(s); Grade 2, isointense lesion(s); Grade 3, hyperintense lesion(s); and Grade 4, combination of lesion types). (3) The presence of contrast material in the biliary system (Grade 0, no excretion; Grade 1, intrahepatic ducts; Grade 2, common duct; and Grade 3, duodenum).

One board-certified abdominal imaging fellow performed region of interest (ROI)-based measurements as follows. For each image set, three ROIs were placed over the hepatic parenchyma in the region of the inferior vena cava (IVC), taking care to avoid large vessels and areas of artifact. Three ROIs were also placed on each of the intrahepatic IVC, right paraspinous muscles, and spleen (when possible; $n = 88$) on the same image as the liver ROIs. Signal intensity ratios (SIRs) were calculated as follows: SIR_{LV} = mean SI_{liver}/mean SI_{IVC}; SIR_{LM} = mean SI_{liver}/mean SI_{muscle}; and SIR_{LS} = mean SI_{liver}/mean SI_{spleen}. Severity of hepatic steatosis was calculated as an estimated signal fat fraction (FF_{est}) from the

Author Manuscript Author Manuscript Author Manuscript Author Manuscript

precontrast in/opposed phase acquisition as $FF_{est} = (k_{in} \times SI_{in} - k_{out} \times SI_{out})/(k_{in} \times SI_{in} + k_{out} \times SI_{out})$, where k_{in} and k_{out} are correction factors for the spectral complexity of fat, derived from previous publications (20).

Statistical Analysis

"Mean phase adequacy" was calculated for each image set as the average of reader grades of each phase adequacy. "Overall phase adequacy" was determined for each image set if at least three readers assigned it a phase adequacy grade of 2 or greater. Using these scores, "time to adequacy" was determined as the postcontrast acquisition time of the first image set to achieve overall phase adequacy by the previously mentioned definition.

Intraclass correlation coefficients (ICCs) were calculated to determine reader agreement for phase adequacy, presence/types of lesions, and degree of biliary ductal enhancement. Correlation testing using the Spearman rank sum test was performed for time to adequacy versus age, total bilirubin, albumin, creatinine, presence of liver lesions, and FF_{est} (per patient basis); and mean phase adequacy versus acquisition time, level of biliary enhancement, SIR_{LV}, SIR_{LM}, and SIR_{LS}, presence of liver lesions, and FF_{est} (per image set basis). Differences in time to adequacy based on gender were tested using the Mann–Whitney *U* test. Area under the receiver operating characteristic (AUROC) curve was calculated and ROC curve analysis performed for the prediction of overall phase adequacy by the acquisition time, level of biliary enhancement, SIR_{LV}, SIR_{LM}, and SIR_{LS}, on a per image set basis. Cumulative adequacy over time was determined as the number of patients who had achieved an overall adequate HP for a given postinjection time.

Finally, a decision rule for stopping an examination was derived using the statistically strongest predictor of adequacy. The rule was tested using the same data sets to determine whether using the rule might have resulted in shorter postcontrast times compared to the standard 20-minute post-contrast stopping rule, using the Spearman rank sum test.

All statistical analyses were performed using SPSS v21 (IBM, Armonk, NY). For all tests, a value of $P < .05$ was considered significant.

RESULTS

Ninety-seven patients met all the inclusion criteria, with a total of 240 qualifying image sets. Patient factors, laboratory values, and FF_{est} values are summarized in Table 1. Indications for MRI included evaluation of focal liver lesion ($n = 26$), and evaluation of metastatic disease ($n = 71$) from the following primary tumors: colorectal ($n = 16$); pancreatic ($n = 14$); breast ($n = 10$); neuroendocrine tumor ($n = 10$); melanoma ($n = 8$); cholangio-carcinoma ($n = 4$); duodenal ($n = 3$); gastrointestinal stromal tumor ($n = 3$); and gallbladder, urinary bladder, or renal (each $n = 1$). No lesions were observed in 25 of 97 cases, whereas 72 examinations demonstrated hypointense ($n = 62$), isointense ($n = 2$), hyperintense ($n = 3$), or a combination of lesions ($n = 5$). Most hypointense lesions were interpreted as cysts based on review of the imaging reports and additional pulse sequences, particularly T2-weighted images.

Author Manuscript Author Manuscript Author Manuscript Author Manuscript

Reader agreement was excellent, with ICCs of 0.88 for the presence/type of liver lesions, 0.91 for phase adequacy, and 0.98 for level of ductal enhancement. Of the 97 patients, 12 (12%) reached an adequate HP by 10 minutes postinjection, 78 (80%) were adequate by 15 minutes, 90 (93%) were adequate by 20 minutes, and 93 (96%) were adequate by 25 minutes (Fig. 1).

There was no statistically significant correlation between time to adequacy and patient age, gender, total bilirubin, creatinine, albumin, or FF_{est} on a per patient basis ($P = .24–.85$).

On a per image set basis, there were correlations between mean phase adequacy and image characteristics as follows, from weakest to strongest correlation: lesion presence ($P = .131$, $r = 0.10$); FF_{est} ($P = .112$, $r = 0.15$); acquisition time ($P < .001$, $r = 0.50$); level of biliary enhancement ($P < .001$, $r = 0.56$); SIR_{LS} ($P < .001$, $r = 0.73$); SIR_{LM} ($P < .001$, $r = 0.73$); and SIR_{LV} ($P < .001$, $r = 0.81$).

For predicting image set adequacy, AUROC values were 0.80 for acquisition time, 0.82 for biliary enhancement, 0.87 for SIR_{LS}, 0.88 for SIR_{LM}, and 0.94 for SIR_{LV} (Fig. 2).

Using the ROC analysis, a threshold of $SIR_{LV} = 1.8$ was found to be the best predictor of ideal stopping time. Because most image sets for which this threshold was reached occurred between 10 and 15 minutes postcontrast injection, the following stopping rule was proposed: stop the examination if $SIR_{LV} \geq 1.8$ on a phase obtained at 10–15 minutes postcontrast injection. Using the existing data set, we found that this threshold would have provided an earlier (compared to standard 20 minutes) stopping of the examination in 54 of 97 (56%) cases. The mean postcontrast time for these shortened examinations was 12:11 ± 1:17, which was significantly shorter than the standard 20-minute time ($P < .001$). Using this stopping rule, none of the examinations that were stopped before 20 minutes would have been inadequate. Finally, incorporating the postcontrast times for these examinations with the remaining examinations that would have normally been stopped at 20 minutes, the mean examination time for all patients would have been 15:39 ± 4:02, again significantly shorter than the standard 20-minute time ($P < .001$).

For ease of use, a simpler stopping rule of $SIR_{LV} \geq 2.0$ was also examined. This would have lead to stopping 37 of 97 (38%) examinations early, with a mean postcontrast time of 12:21 ± 1:15, again significantly shorter than the standard 20-minute time ($P < .001$). Using this stopping rule, none of the examinations that were stopped before 20 minutes would have been inadequate. After incorporating these post-contrast times into the overall cohort, the mean examination time for all patients would have been 17:05 ± 3:43, again significantly shorter than the standard 20-minute time ($P < .001$).

Two representative examples from examinations that could have been halted before 20 minutes postinfusion are shown in Figures 3 and 4.

DISCUSSION

One of the important challenges in the routine use of gadoxetate disodium for routine liver MRI is related to patient throughput (15,21–24). In particular, dynamic postcontrast imaging

Author Manuscript Author Manuscript Author Manuscript Author Manuscript

with extracellular agents can usually be completed 5–8 minutes after contrast media injection, whereas postcontrast imaging with gadoxetate is typically carried out at 20 minutes (9,15,21). Although performing T2-weighted and diffusion-weighted imaging after the late dynamic phase has been described as a way to use the inactive time until the 20-minute delayed phase, at our centers these sequences are typically completed by 10–15 minutes postinjection, and a substantial amount of time is spent simply waiting for the 20-minute phase (23–25).

This study demonstrates that the earliest time at which an adequate HP can be achieved cannot be predicted using patient demographic or laboratory values, in patients without CLD. This is in agreement with numerous other published series, which have found, at best, weak correlation with these factors and gadoxetate uptake. We also investigated whether the presence of liver lesions or parenchymal hypointensity because of hepatic steatosis might influence the readers' assessment of adequacy; however, no such significant correlations were found.

A previous report from Motosugi et al. (26) examined the possibility of shortening postcontrast HP time to 10 minutes in MRI examinations performed to detect metastatic disease. The authors found that an HP delay time of 10 minutes was adequate in most patients, although in a minority of lesions it was well-visualized at 20 minutes but not well-seen at 10 minutes. Motosugi et al. found that the ratio of liver to spleen signal intensity was a strong predictor of phase adequacy. Our results also show that the liver to spleen ratio predicts phase adequacy, but that the liver to vein ratio was more strongly predictive. Because most of the lesions in our study were hypointense in the HP, the stronger performance of SIR_{LV} versus SIR_{LS} suggests that venous signal intensity is a better predictor of hypointense lesion signal intensity than the spleen. Alternatively, SIR_{LS} may have been more strongly affected than SIR_{LV} by regional image intensity/noise variations, which can be the result of parallel imaging, coil sensitivity profiles, image postprocessing, or other causes. Importantly, an SIR was a stronger predictor of adequacy than either postinjection time or biliary enhancement, objective markers that have been previously proposed (27–30). In addition, a decision rule for stopping an examination based on the SIR_{LV} would have provided a shorter mean examination time for more than half of the MRIs in our cohort compared to a standard 20-minute delay. This may serve as a useful guideline for technologists performing MRI examinations to determine whether an adequate phase has been reached before the standard 20-minute postinjection time to improve patient throughput. To simplify the decision rule for routine use by MRI technologists, a decision rule of $SIR_{LV} \geq 2.0$ can also provide significantly shorter examination times.

Other reports examining the appearance of liver lesions have suggested that an adequate HP may be reached at 20 minutes postinjection, with similar performance comparing 10- and 20-minute image sets (14,16). Jeong et al. (16) found that readers detected more hepatic metastases when including hepatocyte data sets, but observed no advantage in using 20-minute data sets over 10-minute data sets. Sofue et al. (14) demonstrated similar image quality between 10- and 20-minute HPs in the setting of colorectal metastases. Both groups observed that liver-to-metastasis SIRs were higher at 20 minutes than at 10 minutes. In addition, it has been repeatedly shown that increasing the T1-weighting of hepatocyte data

Author Manuscript Author Manuscript Author Manuscript Author Manuscript

sets (particularly by increasing the flip angle) can improve contrast between the liver and focal lesions, and in combination with the similar subjective image quality (9–12). It may therefore be possible to reproduce both the diagnostic performance and contrast of a 20-minute HP using an earlier HP combined with strong T1-weighting. In this retrospective clinical study, only images with conventional flip angles were available, because of previous experiences with energy deposition and image noise challenges when using high flip angles at 3 T.

This study has several limitations, including its retrospective design and the use of the opinion of blinded readers to determine HP adequacy. Although many focal lesions were present in our study population, many were thought to represent cysts, and histologic analysis was unavailable for most of the solid lesions. Thus, we did not perform an analysis of lesion conspicuity because it was unclear whether this would be meaningful. In addition, our determinations of estimated liver fat fraction were likely inaccurate, because we did not account for either T1 or T2* effects using two-point in/opposed phase data. Another limitation is that the SIR is dependent on the T1-weighting of the pulse sequence during the HP. Therefore, SIR thresholds may require adjustment for sequences with different weighting across MR scanners and institutions. In this study, only one reader performed SIR measurements; multiple sets of SIR measurements would have allowed us to examine the reproducibility of those measurements. Also, we used a 4-point Likert scale for assessing lesion conspicuity because we felt that four categories of conspicuity were appropriate in this setting; however, 3- and 5-point scales have been described and could have been used. Finally, there is heterogeneity among institutions regarding the dosing of gadoxetate, ranging from the package insert dose (0.025 mmol/kg) to 0.05 mmol/kg, to simple volume dosing (eg, 10 mL) as was performed in our study (16,31–33). Variations in dose could lead to differences in the time at which adequacy of hepatobiliary enhancement is achieved, and could explain the differences in results between this and other studies. Weight-based dosing may lead to more consistent hepatocyte uptake across a range of patient weights. Additional studies examining the effect of dose on the time to adequacy of the hepatobiliary phase may be warranted, particularly for different dosing regimens. In addition, genetic polymorphisms of the organic anion polypeptide transporters can affect the amount of gadoxetate uptake, but genetic data were not available in our study, and we could not account for those effects (34). Finally, this study was limited to patients without a history of CLD. It is well known that patients with cirrhosis often have reduced hepatobiliary uptake (34–36). Separate studies for time to adequacy of patients with CLD are certainly needed.

This study has several strengths. First, a relatively large number of image sets were analyzed. Further, we used four readers practicing at different institutions, and the strong consensus among the readers suggests that these results are generalizable (ICC = 0.88–0.94). In addition, image parameters and quality were uniform and the study population relatively homogeneous, consisting of outpatients undergoing characterization of focal liver lesions or evaluation for metastatic disease without a history of CLD.

Author Manuscript Author Manuscript Author Manuscript Author Manuscript

CONCLUSIONS

Most patients without CLD undergoing gadoxetate-enhanced liver MRI achieve adequate HP at 20 minutes. However, a shorter postcontrast stopping time (15 minutes) can be used in most patients, in the absence of known or potential chronic parenchymal liver disease. The ratio of the signal intensities of the liver to the IVC was the strongest objective predictor of adequacy in this study, and was a better predictor of adequacy than postinjection time or biliary enhancement.

Acknowledgments

SBR receives partial salary support from the NIH (RC1 EB010384).

References

1. Muhi A, Ichikawa T, Motosugi U, et al. Diagnosis of colorectal hepatic metastases: comparison of contrast-enhanced CT, contrast-enhanced US, superparamagnetic iron oxide-enhanced MRI, and gadoxetic acid-enhanced MRI. J Magn Reson Imaging. 2011; 34:326–335. [PubMed: 21780227]
2. Chung WS, Kim MJ, Chung YE, et al. Comparison of gadoxetic acid-enhanced dynamic imaging and diffusion-weighted imaging for the preoperative evaluation of colorectal liver metastases. J Magn Reson Imaging. 2011; 34:345–353. [PubMed: 21702068]
3. Chen L, Zhang J, Zhang L, et al. Meta-analysis of gadoxetic acid disodium (Gd-EOB-DTPA)-enhanced magnetic resonance imaging for the detection of liver metastases. PLoS One. 2012; 7:e48681. [PubMed: 23144927]
4. Mohajer K, Frydrychowicz A, Robbins JB, et al. Characterization of hepatic adenoma and focal nodular hyperplasia with gadoxetic acid. J Magn Reson Imaging. 2012; 36:686–696. [PubMed: 22674623]
5. Grazioli L, Bondioni MP, Haradome H, et al. Hepatocellular adenoma and focal nodular hyperplasia: value of gadoxetic acid-enhanced MR imaging in differential diagnosis. Radiology. 2012; 262:520–529. [PubMed: 22282184]
6. Hyodo T, Murakami T, Imai Y, et al. Hypovascular nodules in patients with chronic liver disease: risk factors for development of hypervascular hepatocellular carcinoma. Radiology. 2013; 266:480–490. [PubMed: 23362095]
7. Bashir MR, Gupta RT, Davenport MS, et al. Hepatocellular carcinoma in a North American population: does hepatobiliary MR imaging with Gd-EOB-DTPA improve sensitivity and confidence for diagnosis? J Magn Reson Imaging. 2013; 37:398–406. [PubMed: 23011874]
8. Motosugi U, Ichikawa T, Morisaka H, et al. Detection of pancreatic carcinoma and liver metastases with gadoxetic acid-enhanced MR imaging: comparison with contrast-enhanced multi-detector row CT. Radiology. 2011; 260:446–453. [PubMed: 21693662]
9. Nagle SK, Busse RF, Brau AC, et al. High resolution navigated three-dimensional T(1)-weighted hepatobiliary MRI using gadoxetic acid optimized for 1. 5 Tesla. J Magn Reson Imaging. 2012; 36:890–899. [PubMed: 22648633]
10. Bashir MR, Husarik DB, Ziemlewicz TJ, et al. Liver MRI in the hepatocyte phase with gadolinium-EOB-DTPA: does increasing the flip angle improve conspicuity and detection rate of hypointense lesions? J Magn Reson Imaging. 2012; 35:611–616. [PubMed: 22034383]
11. Bashir MR, Merkle EM. Improved liver lesion conspicuity by increasing the flip angle during hepatocyte phase MR imaging. Eur Radiol. 2011; 21:291–294. [PubMed: 20686771]
12. Haradome H, Grazioli L, Al manea K, et al. Gadoxetic acid disodium-enhanced hepatocyte phase MRI: can increasing the flip angle improve focal liver lesion detection? J Magn Reson Imaging. 2012; 35:132–139. [PubMed: 21960465]
13. Goodwin MD, Dobson JE, Sirlin CB, et al. Diagnostic challenges and pitfalls in MR imaging with hepatocyte-specific contrast agents. Radiographics. 2011; 31:1547–1568. [PubMed: 21997981]

Author Manuscript Author Manuscript Author Manuscript Author Manuscript

14. Sofue K, Tsurusaki M, Tokue H, et al. Gd-EOB-DTPA-enhanced 3. 0 T MR imaging: quantitative and qualitative comparison of hepatocyte-phase images obtained 10 min and 20 min after injection for the detection of liver metastases from colorectal carcinoma. Eur Radiol. 2011; 21:2336–2343. [PubMed: 21748389]
15. Ringe KI, Husarik DB, Sirlin CB, et al. Gadoxetate disodium-enhanced MRI of the liver: part 1, protocol optimization and lesion appearance in the non-cirrhotic liver. AJR Am J Roentgenol. 2010; 195:13–28. [PubMed: 20566794]
16. Jeong HT, Kim MJ, Park MS, et al. Detection of liver metastases using gadoxetic-enhanced dynamic and 10- and 20-minute delayed phase MR imaging. J Magn Reson Imaging. 2012; 35:635–643. [PubMed: 22095933]
17. Dixon WT. Simple proton spectroscopic imaging. Radiology. 1984; 153:189–194. [PubMed: 6089263]
18. Ma J. Breath-hold water and fat imaging using a dual-echo two-point Dixon technique with an efficient and robust phase-correction algorithm. Magn Reson Med. 2004; 52:415–419. [PubMed: 15282827]
19. Feuerlein S, Boll DT, Gupta RT, et al. Gadoxetate disodium-enhanced hepatic MRI: dose-dependent contrast dynamics of hepatic parenchyma and portal vein. AJR Am J Roentgenol. 2011; 196:W18–W24. [PubMed: 21178026]
20. Reeder SB, Robson PM, Yu H, et al. Quantification of hepatic steatosis with MRI: the effects of accurate fat spectral modeling. J Magn Reson Imaging. 2009; 29:1332–1339. [PubMed: 19472390]
21. Cruite I, Schroeder M, Merkle EM, et al. Gadoxetate disodium-enhanced MRI of the liver: part 2, protocol optimization and lesion appearance in the cirrhotic liver. AJR Am J Roentgenol. 2010; 195:29–41. [PubMed: 20566795]
22. Frydrychowicz A, Lubner MG, Brown JJ, et al. Hepatobiliary MR imaging with gadolinium-based contrast agents. J Magn Reson Imaging. 2012; 35:492–511. [PubMed: 22334493]
23. Muhi A, Ichikawa T, Motosugi U, et al. Diffusion- and T(2)-weighted MR imaging of the liver: effect of intravenous administration of gadoxetic acid disodium. Magn Reson Med Sci. 2012; 11:185–191. [PubMed: 23037563]
24. Ahn SJ, Kim MJ, Hong HS, et al. Distinguishing hemangiomas from malignant solid hepatic lesions: a comparison of heavily T2-weighted images obtained before and after administration of gadoxetic acid. J Magn Reson Imaging. 2011; 34:310–317. [PubMed: 21598345]
25. Kim YK, Kwak HS, Kim CS, et al. Detection and characterization of focal hepatic tumors: a comparison of T2-weighted MR images before and after the administration of gadoxectic acid. J Magn Reson Imaging. 2009; 30:437–443. [PubMed: 19629973]
26. Motosugi U, Ichikawa T, Tominaga L, et al. Delay before the hepatocyte phase of Gd-EOB-DTPA-enhanced MR imaging: is it possible to shorten the examination time? Eur Radiol. 2009; 19:2623–2629. [PubMed: 19471935]
27. Corwin MT, Karam AR, Baker SP, et al. Determination of cystic duct patency using hepatobiliary MRI with gadoxetate disodium: is T1 pre-contrast imaging necessary? J Magn Reson Imaging. 2012; 35:601–606. [PubMed: 22034256]
28. Lee NK, Kim S, Lee JW, et al. Biliary MR imaging with Gd-EOB-DTPA and its clinical applications. Radiographics. 2009; 29:1707–1724. [PubMed: 19959517]
29. Ringe KI, Husarik DB, Gupta RT, et al. Hepatobiliary transit times of gadoxetate disodium (Primovist(R)) for protocol optimization of comprehensive MR imaging of the biliary system—what is normal? Eur J Radiol. 2011; 79:201–205. [PubMed: 20347540]
30. Tschirch FT, Struwe A, Petrowsky H, et al. Contrast-enhanced MR cholangiography with Gd-EOB-DTPA in patients with liver cirrhosis: visualization of the biliary ducts in comparison with patients with normal liver parenchyma. Eur Radiol. 2008; 18:1577–1586. [PubMed: 18369632]
31. Frydrychowicz A, Jedynak AR, Kelcz F, et al. Gadoxetic acid-enhanced T1-weighted MR cholangiography in primary sclerosing cholangitis. J Magn Reson Imaging. 2012; 36:632–640. [PubMed: 22581411]

Author Manuscript Author Manuscript Author Manuscript Author Manuscript

32. Davenport MS, Viglianti BL, Al-Hawary MM, et al. Comparison of acute transient dyspnea after intravenous administration of gadoxetate disodium and gadobenate dimeglumine: effect on arterial phase image quality. Radiology. 2013; 266:452–461. [PubMed: 23192781]

33. Kim MJ, Rhee HJ, Jeong HT. Hyperintense lesions on gadoxetate disodium-enhanced hepatobiliary phase imaging. AJR Am J Roentgenol. 2012; 199:W575–W586. [PubMed: 23096201]

34. Nassif A, Jia J, Keiser M, et al. Visualization of hepatic uptake transporter function in healthy subjects by using gadoxetic acid-enhanced MR imaging. Radiology. 2012; 264:741–750. [PubMed: 22771883]

35. Noren B, Forsgren MF, Dahlqvist Leinhard O, et al. Separation of advanced from mild hepatic fibrosis by quantification of the hepatobiliary uptake of Gd-EOB-DTPA. Eur Radiol. 2013; 23:174–181. [PubMed: 22836161]

36. Sourbron S, Sommer WH, Reiser MF, et al. Combined quantification of liver perfusion and function with dynamic gadoxetic acid-enhanced MR imaging. Radiology. 2012; 263:874–883. [PubMed: 22623698]

Author Manuscript Author Manuscript Author Manuscript Author Manuscript

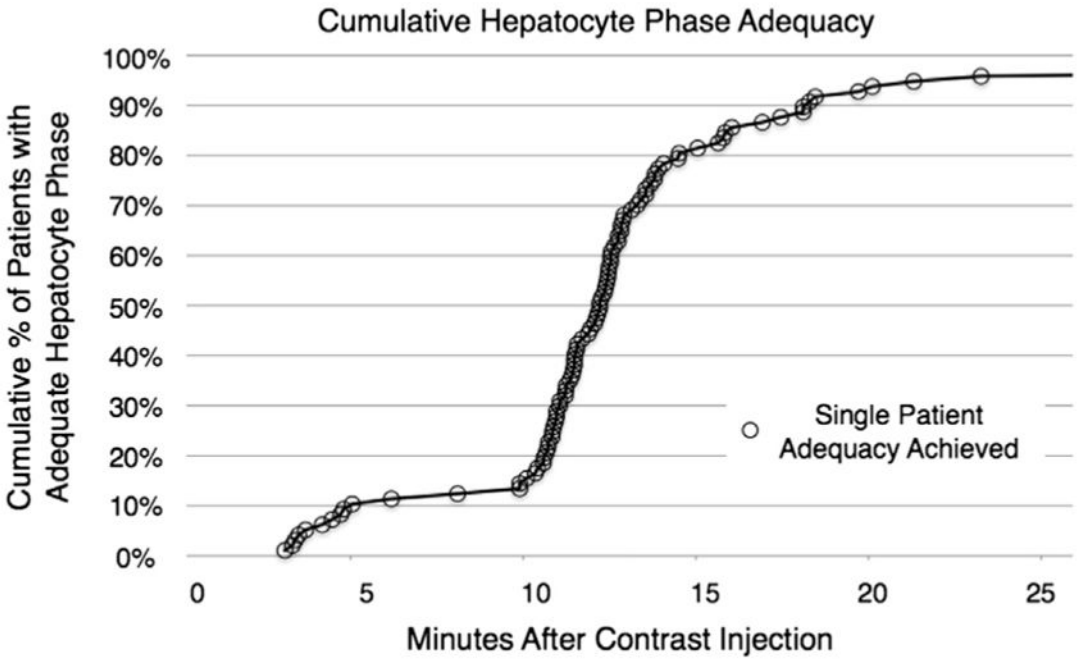

Figure 1.

Cumulative examination adequacy of the hepatobiliary phase over time. Of the 97 patients in this cohort, 12 (12%) reached visual adequacy by 10 minutes, 78 (80%) were adequate by 15 minutes, and 89 (92%) were adequate by 20 minutes.

Author Manuscript Author Manuscript Author Manuscript Author Manuscript

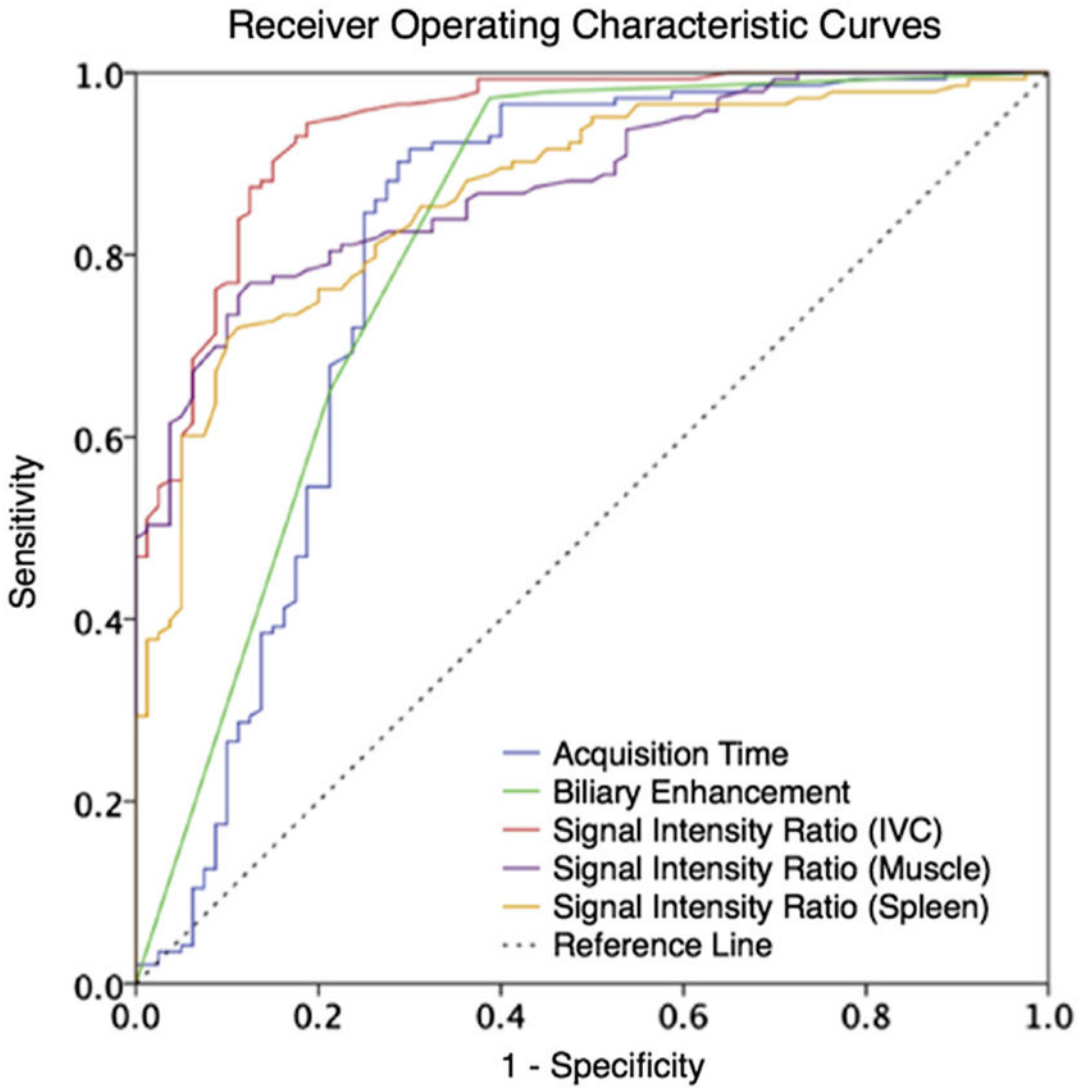

Figure 2.

ROC curves for image characteristics associated with hepatocyte phase adequacy. $SIR_{liver/IVC}$ was the best predictor of phase adequacy (AUROC = 0.94), followed by $SIR_{liver/muscle}$ (AUROC = 0.88), $SIR_{liver/spleen}$ (AUROC = 0.87), biliary enhancement (AUROC = 0.82), and acquisition time (AUROC = 0.80). AUROC, area under the receiver operating characteristic; IVC, inferior vena cava; SIR, signal intensity ratio. (Color version of figure is available online.)

Author Manuscript Author Manuscript Author Manuscript Author Manuscript

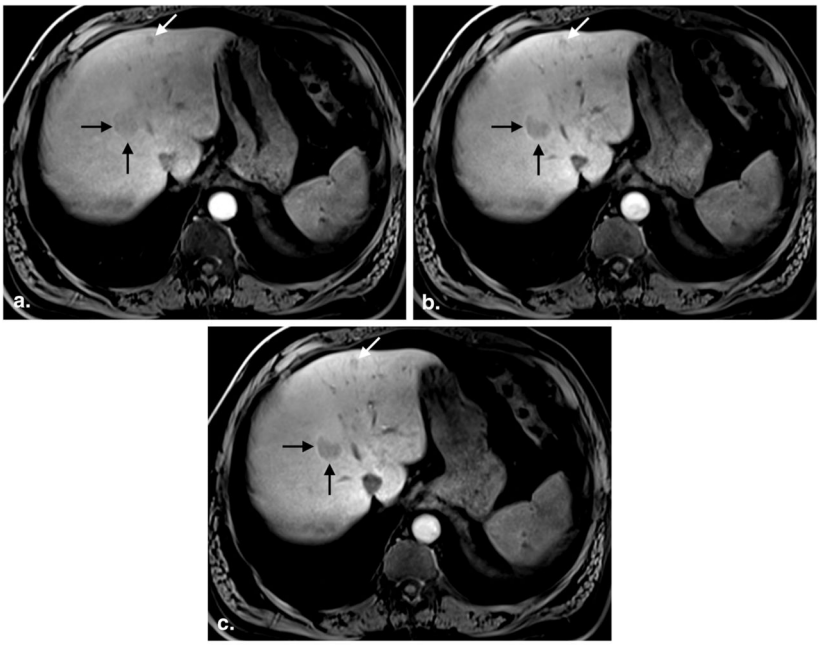

Figure 3.

A 49-year-old man with hepatic adenomas. Three postcontrast images obtained at 3:58 **(a)**, 13:49 **(b)**, and 19:58 **(c)** after gadoxetate injection show progressive hepatic parenchymal enhancement and vessel clearance. The first image set **(a)** was rated an inadequate hepatocyte phase (average reader grade = 1.0, SIR_{LV} = 1.18), whereas the second **(b)** and third **(c)** image sets were rated adequate (average reader grade = 2.0 and 2.0; SIR_{LV} = 1.47 and 1.73, respectively). Note minimal improvement in lesion conspicuity between image set **(b)**, obtained at 13:49, and set **(c)**, obtained at 19:58 postcontrast injection. SIR, signal intensity ratio; LV liver/vein.

Author Manuscript Author Manuscript Author Manuscript Author Manuscript

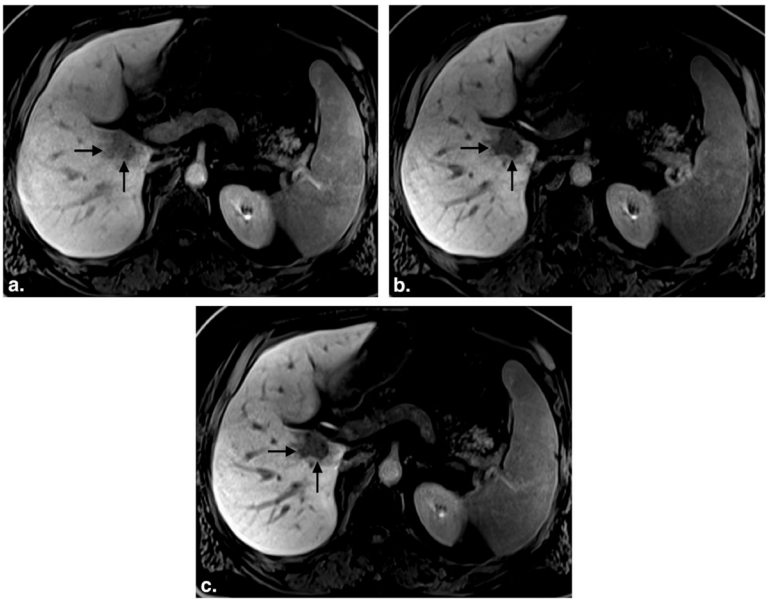

Figure 4.

A 57-year-old man with renal cell carcinoma metastatic to the liver. Three postcontrast images obtained at 3:20 **(a)**, 12:45 **(b)**, and 18:47 **(c)** after gadoxetate injection shows progressive hepatic parenchymal enhancement and vessel clearance. The first image set **(a)** was rated an inadequate hepatocyte phase (average reader score = 1.0, SIR_{LV} = 1.54), whereas the second **(b)** and third **(c)** image sets were rated adequate (average reader score = 2.0 and 2.5; SIR_{LV} = 2.05 and 2.83, respectively). Note minimal improvement in lesion conspicuity between image set **(b)**, obtained at 12:45, and set **(c)**, obtained at 18:47 postcontrast injection. SIR, signal intensity ratio; LV liver/vein.

Author Manuscript

Author Manuscript

Author Manuscript

Author Manuscript

TABLE 1

Descriptive Statistics for the Patient Cohort

Value	Mean ± SD	Range	Number of Patients with Value Available within 4 weeks of MRI
Age (years)	53.7 ± 14.0	28–85	
Gender			31 M; 66 F
Total bilirubin (mg/dL)	0.8 ± 0.3	0.3–1.7	N = 91
Albumin (g/dL)	3.5 ± 0.7	1.8–4.4	N = 91
Serum creatinine (mg/dL)	0.9 ± 0.3	0.5–2.3	N = 95
Estimated liver fat fraction (%)	6 ± 1	0–51	N = 97
Presence of liver lesions	No lesions (n = 25); hypointense lesion(s) (n = 62); isointense lesion(s) (n = 2); hyperintense lesion(s) (n = 3); combination of lesion types (n = 5)		

MRI, magnetic resonance imaging; SD, standard deviation.